Adaptive Chemistry Hot Paper

Deutsche Ausgabe: DOI: 10.1002/ange.201606546
Internationale Ausgabe: DOI: 10.1002/anie.201606546

Adaptive Chemical Networks under Non-Equilibrium Conditions: The Evaporating Droplet

*Joseph J. Armao IV and Jean-Marie Lehn**

Abstract: *Non-volatile solutes in an evaporating drop experience an out-of-equilibrium state due to non-linear concentration effects and complex flow patterns. Here, we demonstrate a small molecule chemical reaction network that undergoes a rapid adaptation response to the out-of-equilibrium conditions inside the droplet leading to control over the molecular constitution and spatial arrangement of the deposition pattern. Adaptation results in a pronounced coffee stain effect and coupling to chemical concentration gradients within the drop is demonstrated. Amplification and suppression of network species are readily identifiable with confocal fluorescence microscopy. We anticipate that these observations will contribute to the design and exploration of out-of-equilibrium chemical systems, as well as be useful towards the development of point-of-care medical diagnostics and controlled deposition of small molecules through inkjet printing.*

The paradigm of creating novel "static" materials, built on persistent chemical bonding patterns, and technologies based on them is giving way to designing dynamic, adaptive materials, incorporating reversible chemical connections, that respond to agents in their environment (physical stimuli or chemical effectors).[1] A crucial step towards developing such novel materials and derived nanotechnologies rests on the elucidation of chemical systems that adapt to out-of-equilibrium conditions so as to produce novel structural, chemical, spatial, and temporal profiles. An evaporating droplet on a surface represents a system where the equilibrium state is perturbed due to a rapid, non-linear evaporation profile.[2] When the contact line of the drop is pinned, evaporation occurs more quickly from the edge of the drop, inducing the formation of outward capillary flows.[3] Suspended solutes within the drop are displaced by these capillary flows leading to the formation of a coffee stain pattern around the periphery.[4] The controlled deposition of solutes from evaporating solutions has been proposed as a nanoscale self-assembly method for a wide range of applications[4b] such as ink jet printing[5] and point-of-care medical diagnostics.[6] The application of this method relies on being able to control whether the coffee stain pattern appears or not. So far, most of the methods used to control the coffee stain effect have relied on heterogeneous colloidal suspensions either by changing their shape,[7] by modifying the surfactant-mediated colloid–colloid interactions,[8] or by altering the capillary flows within the drop.[9] However, the solute constitution in these cases does not change or adapt to the conditions imposed by evaporation.

In contrast, we propose to use homogenous small molecule chemical networks capable of adapting to the out-of-equilibrium environment imposed by the evaporating drop to alter the constitution and deposition pattern of the solutes. Such a responsive system may implement constitutional dynamic chemistry to create chemical networks based on chemical species able to rapidly interconvert by component exchange by virtue of reversible labile bonds.[1a] Adaptation to external physical stimuli can give rise to agonist/antagonist relationships leading to up-regulation and down-regulation of molecules in the network.[10] Here, we demonstrate a system which, during the course of a several minute evaporation time undergoes 1) phase change-induced component selection[11] by selective precipitation of one of the library components triggered by evaporation, 2) rapid self-sorting of the chemical network[12–14] to amplify the appropriate species, 3) dynamics-enabled spatial separation of the precipitating species in the form of a coffee stain pattern, and 4) coupling of the chemical network to chemical concentration gradients induced by capillary flows within the evaporating droplet. In contrast, control chemical sets not displaying the coffee stain effect display neither spatial separation nor coupling to the capillary flows.

Constitutional dynamic networks based on Schiff base imines[15] (Figure 1) were chosen for two reasons: (1) they readily undergo reversible imine formation and exchange processes allowing the formation of constitutional dynamic

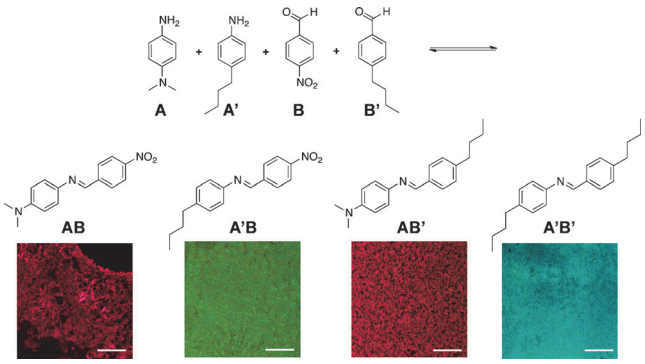

Figure 1. Four-imine chemical library of constituents **AB**, **A'B**, **AB'** and **A'B'**, generated from the four components **A**, **A'**, **B** and **B'**, together with the corresponding solid-state fluorescence of each imine (bottom; scale bar = 45 μm).

[*] Dr. J. J. Armao IV, Prof. Dr. J.-M. Lehn
Institut de Science et d'Ingénierie Supramoléculaires (ISIS)
Université de Strasbourg
8 allée Gaspard Monge, Strasbourg 67000 (France)
E-mail: lehn@unistra.fr

Supporting information for this article can be found under: http://dx.doi.org/10.1002/anie.201606546.

libraries and (2) they display aggregation-induced emission due to a restricted internal rotation mechanism in the solid state.[16] This solid-state fluorescence allows detection of the imines by confocal fluorescence microscopy and avoids the problem of solid-state quenching found with most fluorescent dyes. The fluorescence profile of the imines (Figure 1) was tuned by altering the substitution pattern to incorporate electron-donating and electron-withdrawing groups, with the push–pull imine **AB** displaying the largest fluorescence red-shift ($\lambda = 657$ nm), followed by **AB′** ($\lambda = 643$ nm), **A′B** ($\lambda = 545$ nm), and **A′B′** ($\lambda = 504$ nm; see Figure S1 in the Supporting Information; resolution ± 9.7 nm). Acetonitrile was used as the solvent and the imines were tested for their solubility. Imine **AB** was the least soluble under these conditions with precipitation of the isolated species observed at 3 mM in acetonitrile. The other imines displayed solubilities greater than 50 mM. Deposition of acetonitrile solutions onto a glass surface resulted in a pinned contact line during the evaporation process. The four imines were tested with imine **AB** demonstrating a coffee stain pattern when deposited from unsaturated solutions. The other three imines did not display coffee stain distribution from 10 mM drops due to increased solubility preventing precipitation before complete evaporation (Figure S2).

A two-imine dynamic chemical network consisting of an equimolar mixture of all three components, amines **A** (10 mM) and **A′** (10 mM), as well as aldehyde **B** (10 mM), was equilibrated overnight in acetonitrile under acidic conditions (10 mM DCl) to give an equilibrium mixture containing imines **AB** and **A′B**. Acidic conditions were chosen in order to promote rapid exchange among the network components to ensure an adaptive response. The confocal fluorescence image of an evaporated drop from a 10 mM solution displayed a nearly perfect coffee stain pattern with a fluorescence emission matching that of imine **AB** (Figure 2a). No fluorescence output could be observed corresponding to imine **A′B** indicating its suppression during the evaporation process. Integration of the fluorescence signal over the entire droplet showed a very strong peak centered around 646 nm corresponding to imine **AB** (Figure 2c). In contrast, when a control experiment was performed using a neutral, non-exchanging solution of the separately prepared imines **AB** and **A′B**, the fluorescence signal from imine **A′B** could be clearly distinguished and there was no coffee stain effect observed under these conditions (Figure 2b,d). The fluorescence intensity profile demonstrating the spatial distribution of the imines from the two droplets is displayed in Figure 2e and shows the distribution of almost all of the material at the edges of the drop in the adaptive network and a nearly even distribution throughout the drop with the non-exchanging control sample. The difference in the response of the two droplets is due to the presence of acid in the solution that induces rapid imine exchange allowing the network to adapt to a change in the concentration of one of the components. Under acid catalysis, we observed by ^{1}H NMR spectroscopy very fast exchange kinetics in excess of $1\,M^{-1}s^{-1}$ with a half-life of less than 40 s. Figure 2f shows the comparison of the exchange kinetics versus the evaporation kinetics (see the Supporting Information for details) of an

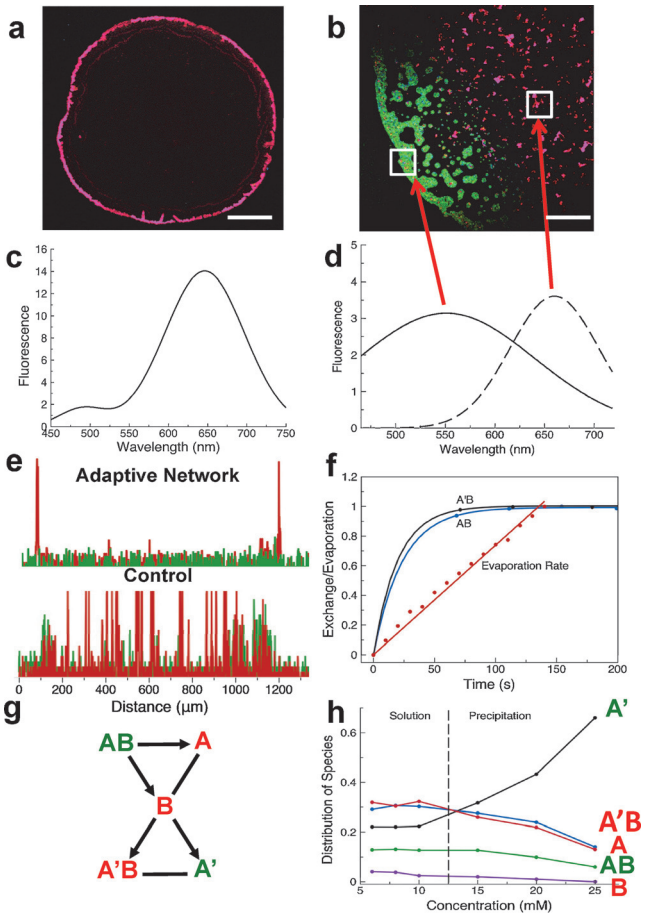

Figure 2. Confocal fluorescence microscope image of a coffee stain produced from the two-imine dynamic network **AB**/**A′B** with and without acid catalysis (a; scale bar = 750 μm, b; scale bar = 250 μm); fluorescence output indicating only imine **AB** has been deposited from solution (c); fluorescence output demonstrating both imines are present in the deposition pattern (d); fluorescence profile from a cross-section of stains formed from evaporated droplets with and without acid catalysis (e, top/bottom; red corresponds to fluorescence emission from **AB** and green with **A′B**); overlay of the imine exchange rate with the evaporation rate of the acetonitrile droplet demonstrating sufficiently fast exchange dynamics under acidic conditions to enact an adaptive response (f); connectivity of the dynamic network formed by precipitating imine **AB** resulting an increase (green) in the amine **A′** and a decrease (red) in all other species (g); ^{1}H NMR solution distribution of species as a function of concentration; above 12 mM precipitation of imine **AB** induces the network response (h). In (c), the shoulder at 500 nm may be attributed to background fluorescence from the substrate.

acetonitrile droplet. Clearly, the exchange process occurs much quicker than the droplet evaporates allowing the self-sorting response of the chemical network to occur. Thermodynamically, the adaptive response may be explained through the connectivity of the network, as shown in Figure 2g. Here, imines **AB** and **A′B** as well as their constituents **A**, **A′**, and **B** are represented with the common aldehyde **B** designated as a hub connecting the two imines. In principle, the increasing concentration in an evaporating drop should lead to (1) the induced precipitation of imine **AB** as it is the least soluble compound, (2) a corresponding decrease in the concentra-

tions of amine **A** and aldehyde **B** as the equilibrium is perturbed in the system, and (3) a secondary response to the decrease in aldehyde **B** leading to a decrease in imine **A′B** and an increase in the amine **A′**. This network configuration was confirmed through ^{1}H NMR experiments on equilibrated solutions at concentrations between 6 mM and 25 mM (equimolar in amines and aldehyde, Figure 2h). Solutions between 6 and 10 mM displayed no precipitation and a consistent distribution of the chemical species: 32% **A**, 29% **A′B**, 22% **A′**, 12% **AB**, 3% **B** (±5%). As the concentration is increased, amine **A′** is amplified in solution while all other species decrease in concentration, confirming the anticipated response of the adaptive network. At 25 mM the distribution of species is around 66% **A′**, 14% **A′B**, 13% **A**, 6% **AB** and 0% **B** (±5%). Meanwhile, analysis of the precipitate confirmed that indeed imine **AB** is the precipitating species (Figure S4).

A four-imine dynamic chemical network was tested by equilibrating a mixture of all four of the amines and aldehydes in Figure 1 (10 mM starting concentration of all species with 10 mM DCl) to give a mixture containing imines **AB**, **A′B**, **AB′**, and **A′B′**. The profile from a 10 mM drop displayed two colors this time, with a tight red band along the periphery and a tail fluorescence in the rest of the deposition profile (Figure 3a). The close-up image and the corresponding fluorescence profiles (Figure 3c,d) demonstrate spatial separation of imines in the deposition profile with the outputs corresponding to imines **AB** and **A′B′**. The distribution of the red color corresponds to the precipitation-induced coffee stain effect already observed with imine **AB**. The deposition of **A′B′** is due to the final evaporation occurring from the center outwards as the remaining solvent adhered to the deposited **AB** along the periphery, with a small amount actually depositing outside the coffee stain pattern. The response of the four-imine constitutional dynamic library (CDL) may be explained by the square [2×2] network connectivity in Figure 3b and the full network, including the component aldehydes and amines, in Figure S5. Precipitation of imine **AB** induces a rapid self-sorting response resulting in the amplification of imines **AB** and **A′B′**. The antagonist relationship with imines **A′B** and **AB′** leads to the decrease in available species **A** and **B** through the re-equilibration due to precipitation of **AB**. The result is an increase in the available species **A′** and **B′** in solution leading to the formation of **A′B′** in an agonist amplification process.[17] ^{1}H NMR experiments confirmed this thermodynamic driving force at different concentrations with the precipitation of imine **AB** from the mixture and the subsequent solution amplification of imine **A′B′** (Figure 3e and Figure S6). The spatial separation of the imines indicates that there is a situation in which the precipitating imine **AB** is being constantly driven by capillary flows towards the droplet edge, where it then deposits. The rest of the solution adapts to the changing distribution resulting in amplification of imine **A′B′** which, due to its high solubility, remains homogenously dissolved in the solution until evaporation is complete. Control over the spatial distribution of imines could be affected by the addition of DMSO to the solutions. A comparison of the radial profile of evaporated droplets from 10 mM solutions with 1% DMSO and 4% DMSO are shown in Figure 3 f,g,h, and S7. Clearly, the 4% DMSO solution provides enough solubility of imine **AB** to cancel out any anisotropy in the deposition pattern. Remarkably the separation observed is a true solution separation of species enacted in a lateral direction and differs from standard precipitation, which should induce no spatial preference for deposition, as well as from usual molecular separation methods implementing an interaction with a substrate medium (i.e. thin layer chromatography, column chromatography, electrophoresis, etc.). This effect also differs from separation of colloids based on size at the periphery of an evaporating droplet.[18]

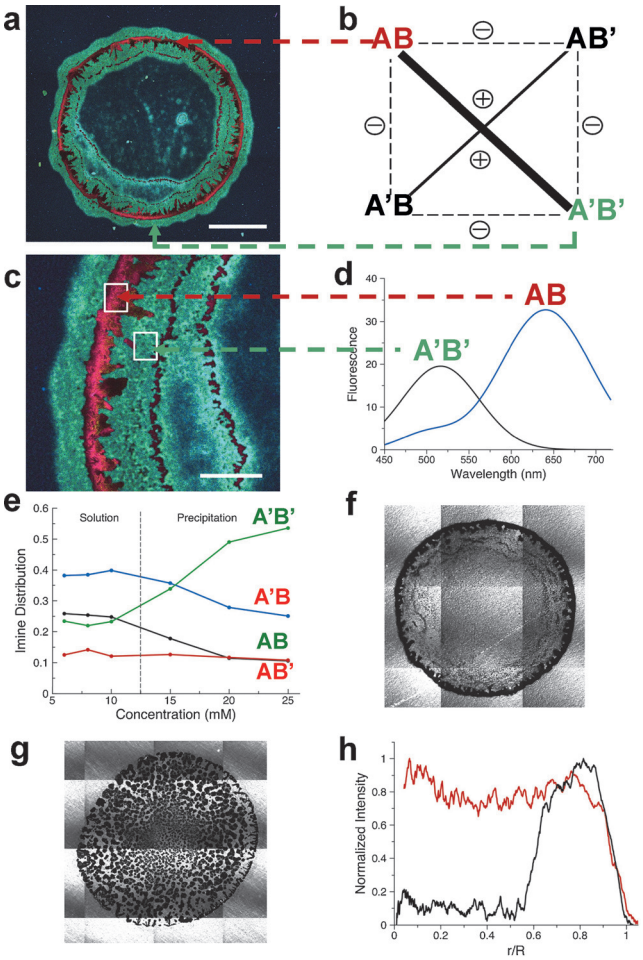

Figure 3. Coffee stain pattern from the four imine network of constituents **AB**, **AB′**, **A′B** and **A′B′** (a; scale bar = 600 μm) and the agonistic/antagonistic relationships in the network leading to the amplification of imines **AB** and **A′B′** (b). A close-up of the ring structure showing the distribution of imines (c; scale bar = 200 μm) and the corresponding fluorescence signals of the regions corresponding to **AB** and **A′B′** (d), as well as imine distribution showing agonistic amplification of **A′B′** upon the precipitation of **AB** (e). Brightfield microscope image of coffee stain pattern with 1% DMSO (f) and 4% DMSO (g) and an overview of the radial profile of each (h; black = 1% DMSO, red = 4% DMSO).

The coffee stain effect is driven by capillary flows within the evaporating droplet and implies the formation of a concentration gradient of the species that is being transported to the periphery—with a lower concentration present in the

center of the drop and a higher concentration present towards the edge. The response of the two-imine network to the presence of a concentration gradient within the evaporating drop was probed by altering the composition of the network to nullify the coffee stain effect. For reference, a close-up image of the stain periphery from the 10 mM experiment reported above is shown in Figure 4a containing only imine

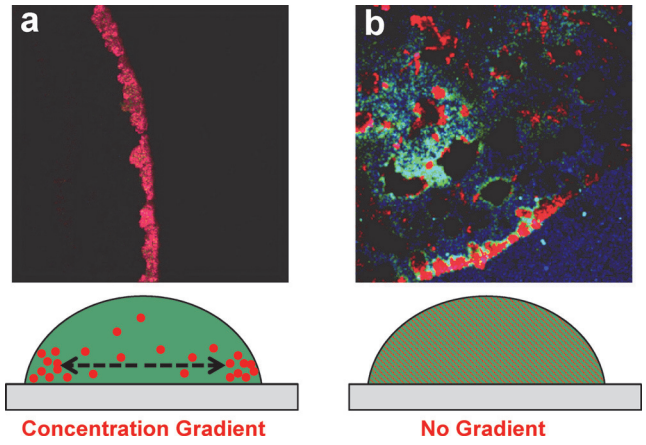

Figure 4. Comparison of two imine network depositions from a 10 mM solution leading to an increased formation of imine **AB** due to the formation of a concentration gradient driven by capillary flows within the droplet (a) and the deposition pattern from a 12 mM solution exhibiting significant deposition of imine **A′B** (green) due to the lack of a concentration gradient (b).

AB. In comparison, deposition from a 12 mM solution containing precipitated **AB** resulted in the deposition of imine **A′B** as witnessed by the green fluorescence in Figure 4b. Here, the presence of the precipitate nullifies the coffee stain effect and destroys the presence of a concentration gradient. The deposition of **A′B** could also be observed from 10 mM solutions containing 4% and 8% added water which disrupted even further the coffee stain effect (Figures S8 and S9). These results clearly demonstrate that the chemical network responds to the formation of a concentration gradient by increasing the formation of imine **AB** as compared to cases where there is no concentration gradient. Importantly, this demonstrates the ability to couple the chemical network to the concentration gradient within the droplet.

Overall, these experiments demonstrate an adaptive response of a chemical network to the out-of-equilibrium conditions in an evaporating droplet resulting in (1) a change in the molecular constitution of the species in the network, (2) a coffee stain effect for the 2-imine chemical network, (3) spatial separation of imine constituents in a 4-imine network, and (4) coupling the network behavior to concentration gradients inside the droplet. These effects are driven by the different solubilities of the molecular species and the rapid ability of the network to re-adjust in response to being perturbed from equilibrium. The present results have implications for the further design of artificial molecular networks operating out-of-equilibrium in response to an anisotropic physical agent (here evaporation of a droplet) as well as towards the development of rapid analytical tools, such as point-of-care medical diagnostic devices.

Acknowledgements

We thank Dr. Annie Marquis for preliminary experiments implementing evaporating drops and Professor Luisa de Cola for use of the confocal fluorescence microscopy apparatus. This work was supported by the ERC Advanced Grant SUPRADAPT (290585).

Keywords: chemical reaction networks · coffee stain effect · droplet · imines · non-equilibrium

How to cite: *Angew. Chem. Int. Ed.* **2016**, *55*, 13450–13454
Angew. Chem. **2016**, *128*, 13648–13652

[1] a) J.-M. Lehn, *Angew. Chem. Int. Ed.* **2015**, *54*, 3276–3289; *Angew. Chem.* **2015**, *127*, 3326–3340; b) I. R. Epstein, B. Xu, *Nat. Nanotechnol.* **2016**, *11*, 312–319; c) J. J. Armao, M. Maaloum, T. Ellis, G. Fuks, M. Rawiso, E. Moulin, N. Giuseppone, *J. Am. Chem. Soc.* **2014**, *136*, 11382–11388; d) E. Mattia, S. Otto, *Nat. Nanotechnol.* **2015**, *10*, 111–119; e) P. T. Corbett, J. Leclaire, L. Vial, K. R. West, J.-L. Wietor, J. K. M. Sanders, S. Otto, *Chem. Rev.* **2006**, *106*, 3652–3711.
[2] Y. O. Popov, *Phys. Rev. E* **2005**, *71*, 036313.
[3] H. Hu, R. G. Larson, *J. Phys. Chem. B* **2002**, *106*, 1334–1344.
[4] a) R. D. Deegan, O. Bakajin, T. F. Dupont, G. Huber, S. R. Nagel, T. A. Witten, *Nature* **1997**, *389*, 827–829; b) W. Han, Z. Lin, *Angew. Chem. Int. Ed.* **2012**, *51*, 1534–1546; *Angew. Chem.* **2012**, *124*, 1566–1579; c) M. Anyfantakis, D. Baigl, *ChemPhysChem* **2015**, *16*, 2726–2734.
[5] J. Sun, B. Bao, M. He, H. Zhou, Y. Song, *ACS Appl. Mater. Interfaces* **2015**, *7*, 28086–28099.
[6] Y. Li, Z. Zhao, M. L. Lam, W. Liu, P. P. Yeung, C.-C. Chieng, T.-H. Chen, *Sens. Actuators B* **2015**, *206*, 56–64.
[7] P. J. Yunker, T. Still, M. A. Lohr, A. G. Yodh, *Nature* **2011**, *476*, 308–311.
[8] a) V. L. Morales, J.-Y. Parlange, M. Wu, F. J. Pérez-Reche, W. Zhang, W. Sang, T. S. Steenhuis, *Langmuir* **2013**, *29*, 1831–1840; b) M. Anyfantakis, D. Baigl, *Angew. Chem. Int. Ed.* **2014**, *53*, 14077–14081; *Angew. Chem.* **2014**, *126*, 14301–14305.
[9] S. N. Varanakkottu, M. Anyfantakis, M. Morel, S. Rudiuk, D. Baigl, *Nano Lett.* **2016**, *16*, 644–650.
[10] a) N. Giuseppone, J.-L. Schmitt, E. Schwartz, J.-M. Lehn, *J. Am. Chem. Soc.* **2005**, *127*, 5528–5539; b) N. Hafezi, J.-M. Lehn, *J. Am. Chem. Soc.* **2012**, *134*, 12861–12868; c) G. Vantomme, S. Jiang, J.-M. Lehn, *J. Am. Chem. Soc.* **2014**, *136*, 9509–9518.
[11] a) P. N. W. Baxter, J.-M. Lehn, K. Rissanen, *Chem. Commun.* **1997**, 1323–1324; b) C.-F. Chow, S. Fujii, J.-M. Lehn, *Chem. Commun.* **2007**, 4363–4365; c) A. Ciesielski, M. El Garah, S. Haar, P. Kovaříček, J.-M. Lehn, P. Samorì, *Nat. Chem.* **2014**, *6*, 1017–1023.
[12] a) R. C. Lirag, K. Osowska, O. S. Miljanic, *Org. Biomol. Chem.* **2012**, *10*, 4847–4850; b) K. Osowska, O. Š. Miljanić, *Angew. Chem. Int. Ed.* **2011**, *50*, 8345–8349; *Angew. Chem.* **2011**, *123*, 8495–8499; c) C.-W. Hsu, O. Š. Miljanić, *Angew. Chem. Int. Ed.* **2015**, *54*, 2219–2222; *Angew. Chem.* **2015**, *127*, 2247–2250.
[13] For kinetic self-sorting see: a) P. Mukhopadhyay, P. Y. Zavalij, L. Isaacs, *J. Am. Chem. Soc.* **2006**, *128*, 14093–14102; b) F. Schaufelberger, O. Ramström, *J. Am. Chem. Soc.* **2016**, *138*, 7836–7839.

[14] For supramolecular self-sorting, see: a) M. M. Safont-Sempere, G. Fernandez, F. Würthner, *Chem. Rev.* **2011**, *111*, 5784 – 5814; b) C. Bohne, *Chem. Soc. Rev.* **2014**, *43*, 4037 – 4050.
[15] a) M. E. Belowich, J. F. Stoddart, *Chem. Soc. Rev.* **2012**, *41*, 2003 – 2024; b) for a review on Schiff bases, see for instance: T. T. Tidwell, *Angew. Chem. Int. Ed.* **2008**, *47*, 1016 – 1020; *Angew. Chem.* **2008**, *120*, 1032 – 1036.
[16] J. Mei, N. L. C. Leung, R. T. K. Kwok, J. W. Y. Lam, B. Z. Tang, *Chem. Rev.* **2015**, *115*, 11718 – 11940.
[17] J.-M. Lehn, *Angew. Chem. Int. Ed.* **2013**, *52*, 2836 – 2850; *Angew. Chem.* **2013**, *125*, 2906 – 2921.
[18] a) C. Monteux, F. Lequeux, *Langmuir* **2011**, *27*, 2917 – 2922; b) D. Noguera-Marín, C. L. Moraila-Martinez, M. A. Cabrerizo-Vilchez, M. A. Rodrihuez-Valverde, *Langmuir* **2015**, *31*, 6632 – 6638.

Received: July 6, 2016
Revised: August 1, 2016
Published online: September 26, 2016

